CMEs and frequency cutoff of solar bursts

Aleksander Stanislavsky[1,2], Aleksander Konovalenko[1], Artem Koval[1], Yaroslav Volvach[1], Philippe Zarka[3]

[1] Institute of Radio Astronomy, National Academy of Sciences of Ukraine, Kharkiv, Ukraine;
[2] V.N. Karazin Kharkiv National University, Kharkiv, Ukraine;
[3] LESIA, Observatoire de Paris, CNRS, France;

E mail (a.a.stanislavsky@rian.kharkov.ua).

Accepted: 29 February 2016

Abstract. Radio observations of solar bursts with high-frequency cutoff by the radio telescope UTR-2 (near Kharkiv, Ukraine) at 8-33 MHz on 17-19 August 2012 are presented. Such cutoff may be attributed to the emergence of the burst sources behind limb of the Sun with respect to an observer on the Earth. The events are strongly associated with solar eruptions occurred in a new active region. Ray tracing simulations show that the CMEs play a constructive role for the behind-limb bursts to be detected in ground-based observations. Likely, due to tunnel-like cavities with low density in CMEs, the radio emission of behind-limb solar bursts can be directed towards the Earth.

Keywords: Coronal mass ejection, Radio bursts, Decameter range, High-frequency cutoff.

Introduction

Coronal mass ejections (CMEs) tightly are associated with three types of low-frequency radio bursts (Gopalswamy, 2010), namely II, III and IV types. The bursts mirror the processes that initiate and develop phenomena accompanying CMEs. In particular, type III bursts are produced by the accelerated electrons propagating along open magnetic field lines, type IV ones are associated with energetic electrons trapped in magnetic arches, whereas the type II ones are emitted by electrons accelerated in shocks. Consequently, each type of the bursts has visibly a different frequency-drift rate on dynamical spectra of radio observations. Of the sporadic radio emission from the Sun, the type III bursts are likely most indicative of eruptions of energetic particles (Cane et al., 2002). They provide important diagnostics of the ambient medium through which the solar disturbances travel and can be used as natural plasma probes traversing the corona. Note that our understanding of the bursts and their relations to CMEs are far from perfect.

Although type III bursts are observed from several GHz to tens kilohertz, they do not always show a continuous frequency drift from the highest frequencies to very low ones. The low-frequency cutoff of solar bursts in the ground-based observations is imposed by the ionosphere. As it is well known (see, for example, Alvarez et al., 1972), the type III bursts observed at metric wavelengths often were not detected in the decametric range. It also happens that other bursts of this type appear at decametric wavelengths, but they do not have a continuation at hectometric and longer wavelengths. The causes of this phenomenon can be different: i) influence of a directivity of the radiation, ii) intrinsic features of the radiation mechanism, iii) propagation effects between the source and the observer. The question of what actually happened in a particular case remains open.

In this report we consider the experimental study of solar bursts with high-frequency cutoff at decametric wavelengths, and the cutoff origin is discussed in the context of propagation effects.

Observations

The observations have been conducted by means of the T-shaped Radio Telescope UTR-2 (Braude et al., 1978). The instrument (49º39' N, 36º56' E) is located around 70 km from Kharkiv, Ukraine. Its antenna array consists of 2040 wideband horizontal dipoles forming two array arms: larger (1440 dipoles) has about 1860 m length in north-to-south direction (and 53 m breadthwise), and another (600 dipoles) spreads in east-to-west direction over 900 m (and 39.3 m across). Although the antenna was built early in the 1970s, the regular upgrade of the UTR-2 allowed us incessantly to improve facilities for the study of solar bursts at decameter wavelengths. During this observation the UTR-2 radio telescope was operated in the mode including four sections of the north-south array of the antenna. The total effective area of this antenna configuration is 50 000 m^2 with the beam pattern size of 1°×15° at 25 MHz.

On 17-19 August of 2012 we observed some tens of solar bursts with high-frequency cutoff. Their frequency of cutoff varied from event to event in the range from 14 MHz to the upper observation frequency available for UTR-2, and the frequency drift rate was from 0.3 MHz/s up to some ones MHz/s that are not typical for both ordinary type II and type III solar bursts at decameter wavelengths (see, for example, Mel'nik et al., 2004; Melnik et al., 2010 and references therein). It should be noticed that sometimes the bursts with high-frequency cutoff demonstrate fine structures similar to bright filaments with a small frequency drift rate, and the dynamic radio spectra of such bursts have a quite intricate shape. Therefore, they were even named "caterpillar" in Melnik et al. (2014). The bursts with high-frequency cutoff are characterized by a relatively low degree of polarization about 10 % (Brazhenko et al., 2015) that points out to their genesis at the second harmonic relative to the local plasma frequency. The polarization observations were carried out independently in the radio telescope URAN-2 located near Poltava at the same time. Figure 1 shows the dynamic radio spectra of some events observed in UTR-2 on 18 August of 2012. The data were recorded by the digital DSP spectrometer operating in the frequency range of 8-33 MHz with the frequency-time resolution in 4 kHz and 100 ms, respectively. In particular, the burst at 08:16 UT (bottom panel of Figure 1) had the frequency drift rate about -0.46 MHz/s, and the noticeable frequency of cutoff was 16. ± 1 MHz, although some weak details of radio emission occurred at higher frequencies. Its flux achieved 240 s.f.u. (recall that 1 s.f.u. = 10^{-22} W/(Hz m^2)). In this event we can distinguish two components. One of them has the duration about 20 s at 10 MHz and 8 s at 16 MHz, and the second component lasts 14 s. The properties are confirmed by simultaneous radio observations of the URAN-2 telescope (Brazhenko et al., 2015). In general, the characteristic features of these bursts on 18 August of 2012 were the following: 1) their average half-power duration was about 17.5 s in comparison with 8-9 s in the type III bursts at this frequency range; 2) the frequency drift rate of the bursts was lying in the range between 0.81 MHz/s and 0.34 MHz/s which were lower in several times than these values in ordinary type III bursts; 3) the bursts were moderate in flux (about hundreds s.f.u.). It should be noticed that the bursts with high-frequency cutoff, detected in the UTR-2 observations, did not continue above 33 MHz. This has been checked by means of the corresponding high-frequency observations performed on the Nançay Decametric Array.

On 17-19 August of 2012 many C-class and M-class X-ray flares, following each other, were observed by STEREO, GOES and SOHO spacecrafts (see Figure 2). The solar activity was also accompanied with CMEs. They emerged near the NOAA active region 11548 invisible from the Earth, but it was visible from the STEREO Behind spacecraft.

Problem

In the upper corona, where the solar radio emission in the decametric range arises, the local plasma frequency is substantially greater than the local electron gyrofrequency (see, for example, Stanislavsky et al., 2015). Thus, the magnetic field at these heights, where the exciter of plasma emission propagates, is not strong enough to change the direction of source motion and induce the high-frequency cutoff. The most plausible explanation of this cut-off lies in propagation effects of radio emission between the source and the observer, and their occurrence has reasons. Firstly, according to STEREO observations the solar activity was connected with solar spots on the far side of the Sun relative to the Earth. Secondly, the solar events were associated with many flares and CMEs. They can generate numerous type III solar bursts and various conditions for their propagation between burst sources and terrestrial observers.

The simplest interpretation of the bursts with cutoff has been suggested by Melnik et al. (2014). It is based on an assumption that their radiating sources are located on the far side of the Sun relative to an observer on Earth, and the bursts are emitted at the second harmonic of the local plasma frequency. Then the high-frequency radiation part is hidden (occulted) by the solar corona. However, this concept requires a detailed study. The point is that the refraction of radio emission in coronal plasma plays an important role for solar bursts. Due to this effect, the ray tracing from the behind-limb burst sources may be directed away from the Earth.

Indeed, from the refractive index variation with height in the solar corona, the path of a radio ray is calculated with help of the Snell's law (Bracewell and Preston, 1956; Thejappa and MacDowall, 2010). Without loss of generality, we assume the spherical symmetry of electron density in solar corona that simplifies the ray tracing analysis. In this case the Snell's law takes the form

$$\rho n \sin \varphi = a, \tag{1.1}$$

where φ denotes the angle between the radius-vector from the solar disc center to a ray position point and the tangent to the ray trajectory. Here the refractive index $n(\rho)$ is described by the relation $n^2 = 1 - f_{pe}^2 / f^2$, where f is the frequency of radio emission, $f_{pe} = 8.98(N_e)^{1/2}$the electron plasma frequency in kHz, and N_e (cm^{-3}) defines the electron density of the solar corona in dependence of the distance ρ from the center of the Sun. According to Bracewell and Preston (1956), the point (ρ, θ) of the ray tracing position (in polar coordinates) obeys the equation

$$\theta = a\int_{\rho}^{\infty}\frac{d\rho}{\rho\sqrt{n^2\rho^2 - a^2}}, \tag{1.2}$$

where a is the distance of the asymptote of the ray for large values ρ (with n = 1) from the parallel line through the Sun's center. Here θ is the angle between the line through the center of the Sun, parallel to the asymptote, and the direction on the ray position (Bracewell and Preston, 1956). The turning point of a ray satisfies

$$\rho_a n_a = a, \quad \theta_a = a\int_{\rho_a}^{\infty}\frac{d\rho}{\rho\sqrt{\rho^2 n^2 - a^2}}. \tag{1.3}$$

It is not difficult to show that a ray with frequency f reaches to the solar corona height with $f_{pe} = f$ only, if a is close to zero. Otherwise, the ray is reflected higher than the height with f_{pe}. This means that the refraction of radio emission in the corona model does not allow observing the behind-limb bursts by ground-based instruments (see computer simulations in Figure 3a). Consequently, the value $\theta \geq \pi/2$ requires a special

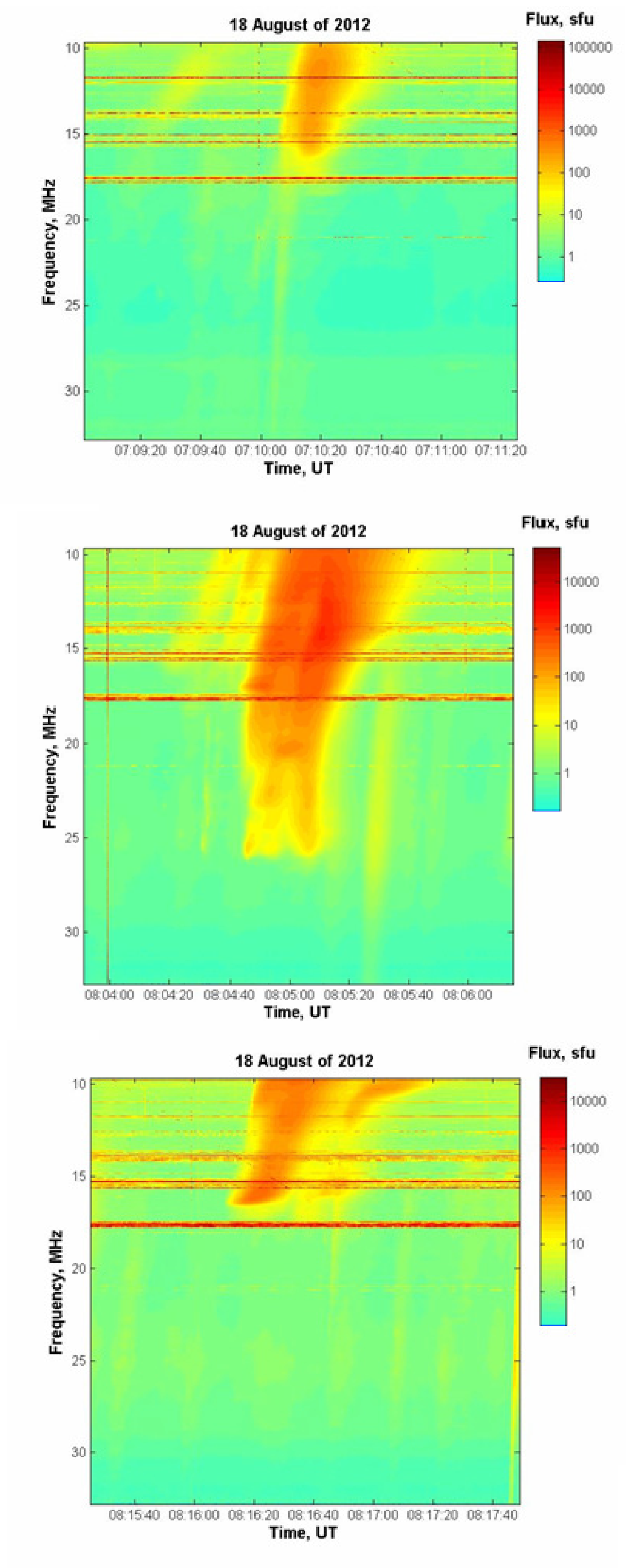

Figure 1 Illustrative examples of the bursts with high-frequency cut-off on 18 August of 2012. The horizontal bright lines on the dynamic spectrum indicate intensive disturbances due to broadcast radio stations.

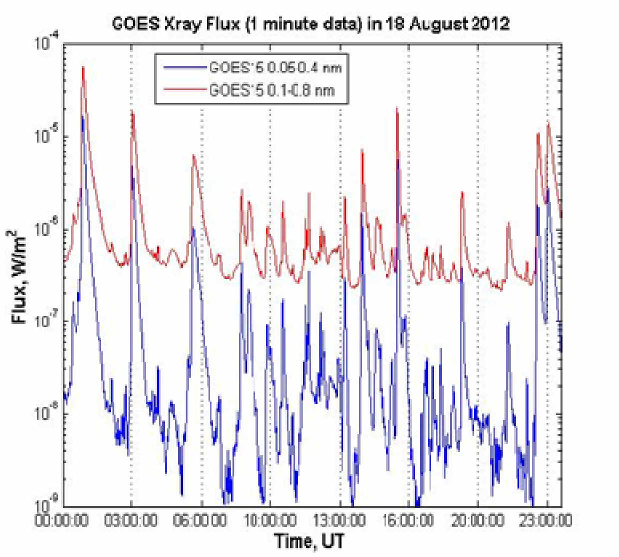

Figure 2 Time series of solar X-ray emission observed by the GOES-15 on 18 August of 2012.

case of the electron density variation with height in the solar corona, something like "coronal" waveguide, where the refractive index would be less than in ambient coronal plasma. Therefore, the scheme of propagation of post-limb radio emission in solar corona (if it is watched on the Earth) should be developed in a new way. As applied to this problem, we pay attention to CMEs that took place near the solar limb. Their occurrence is strongly correlated with the emergence of solar bursts with high-frequency cutoff.

In addition to the CME scenario, the solar radiation from the far side of the Sun could be "delivered" to the observer by means of scattering off turbulent fluctuations of the coronal plasma. However, the cut-off edges of the bursts along frequency (i.e. frequency profile) on the dynamic spectra were too sharp rather than diffusive. This indicates more in favor of the CME scenario. Note also that the fine structure of solar decametric type II radio bursts in the form of drifting narrowband fibers on the dynamic spectrum can be explained in terms of refractive effects due to the inhomogeneous structure of CMEs (Afanasiev, 2009).

Results

As a CME emerges, it typically contains a lower-density cavity behind its crest (dark bands at SOHO LASCO frames, see Figure 4), and it often has a bright prominence core embedded within it (Gibson et al., 2010). Really, following the argument of Aschwanden (2005), the CME density n_{CME} is determined by the observed brightness temperature T_B, namely

$$T_B \approx 0.2 T_e^{-1/2} f^{-2} L n_{CME}^2, \qquad (1.4)$$

where T_e is the electron temperature in solar corona, L the linear dimension of the CME along the line-of-sight. The interesting feature of CMEs indicates that they may form tunnel-like cavities with low density. Under appropriate conditions this permits burst sources, moving behind the solar limb (relative to an observer on the Earth), to send radio signals towards the Earth through and/or due to such cavities. This concept has been verified successfully by computer simulations (Figure 3b). As a model of tunnel-like cavities, we have taken a ring sector, where the electron density in ten times less than in ambient plasma. The inner radius of this ring was taken 2.15 in solar radius, and the external radius is 3.4 solar radii. The center of this ring coincides with the center of the solar limb (circle). The sector covers a corner of the ring from 5º (near the radiation source moving along a radius and generating at the second harmonic relative to the local plasma frequency) to 70º. Due to the low-density cavity, the radio rays of behind-limb bursts move to the Earth, whereas without "coronal" waveguides the radio emission of the bursts is rejected away from the Earth.

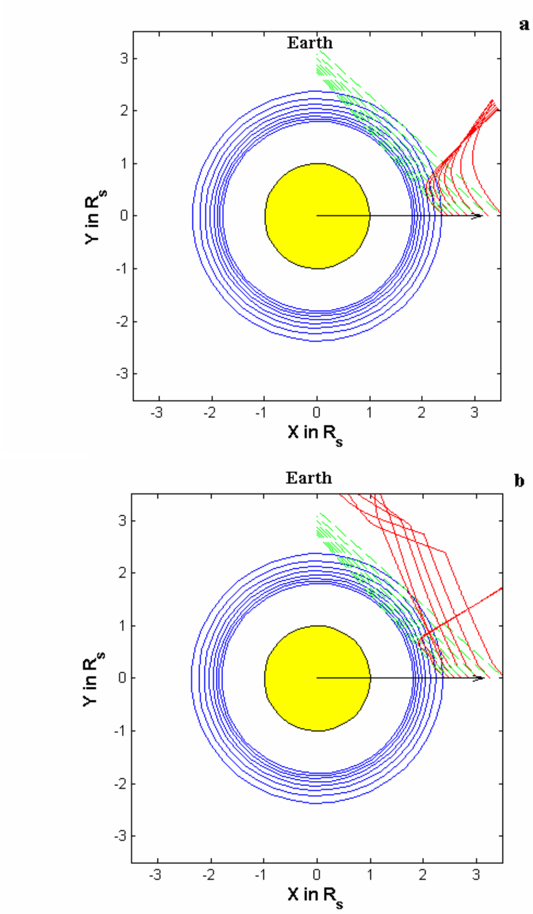

Figure 3 Computer simulations of ray tracing for the spherically symmetric model of the electron density in solar corona: a) without CMEs; b) in the presence of a low-density cavity due to a CME. Axes are in solar radii, and the yellow circle is the Sun. Blue circles mark the coronal heights with plasma frequencies of 15 to 30 MHz in steps of 2 MHz. Rays are shown in red, the black bold arrow indicates the movement of the radiation source (generating at the second harmonic relative to the local plasma frequency), the dashed lines show the tangents to the circles toward the Earth. Due to the low-density cavity, the rays of behind-limb bursts move to the Earth, whereas without CMEs the rays are rejected away from the Earth. As a result, there is an effect of cutoff.

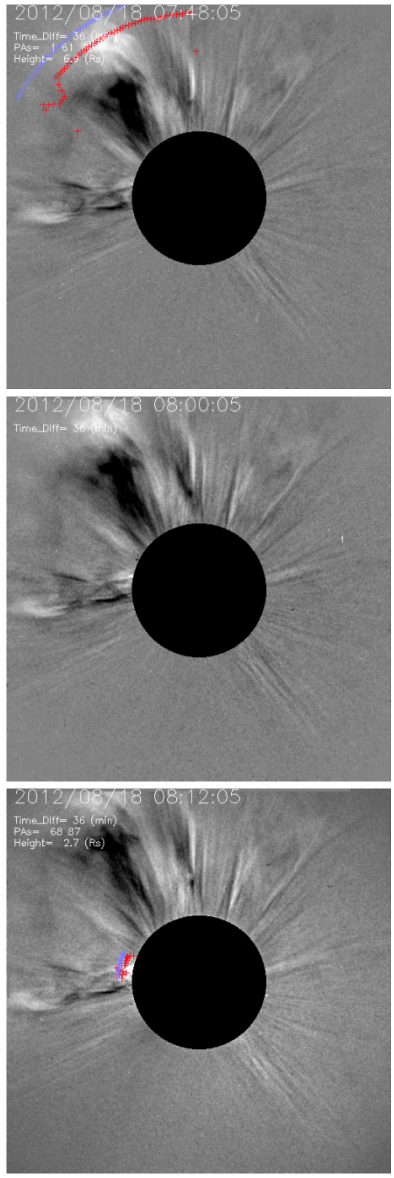

Figure 4 Images of the solar corona, taken by the LASCO coronagraph (C2) on the SOHO observatory at 07:48 UT, 08:00 UT and 08:12 UT (from top to bottom) on 18 August of 2012. The red and blue lines indicate the position of the leading edge using different techniques. Image courtesy of the SOHO team.

As a result, there is an effect of cutoff. Very likely, it is that the radiation is observed in ground-based observations as solar bursts with high-frequency cutoff on 17-19 August of 2012.

Based on the observations, we conclude that the bursts with high-frequency cutoff may be relevant to the type III radio bursts. This is justified by some factors. Firstly, the type III is the largest population of solar bursts. Secondly, the velocity of CMEs is about one hundred times smaller than the speed of electron beams responsible for the type III bursts. Thus, during a solar storm of behind-limb bursts, some of them can get in such a low-density cavity, and hence they will be received at the Earth. In addition to high-frequency cut-off these bursts have at least two other peculiarities, a lower frequency drift rate and a broader temporal profile (at a fixed frequency) in comparison with the ordinary type III burst. Since their source is located behind the solar limb toward the Earth, the effects of radio wave propagation in tunnel-like cavities of the solar corona can distort the observed frequency-drift rate of the bursts. This explains also why the behind-limb bursts have appreciable variations in frequency-time properties so that a part of them is similar to features of type III radio bursts, and others are not. Thus, the CME scenario to explain features of the bursts with high-frequency cutoff is the most plausible one.

Acknowledgments

We would like to thank the GOES, STEREO and SOHO teams for developing and operating the instruments and we are grateful for their open data policy. This research was partially supported by Research Grant 0115U004085 from the National Academy of Sciences of Ukraine.

References

Afanasiev, A. N.: 2009, Ann. Geophys. 27, 3933(doi: 10.5194/angeo-27-3933-2009).

Alvarez, H., Haddock, F., and Lin R.P.: 1972, Solar Phys. 26, 468(doi: 10.1007/BF00165288).

Aschwanden, M.: 2005, Physics of the Solar Corona: An Introduction with Problems and Solutions, Springer Praxis Books, Chichester, 924 p.

Bracewell, R.N., Preston, G.W.: 1956, Astrophys. J. 123, 14(doi: 10.1086/146125).

Braude, S.Ya., Megn, A.V., Ryabov, B.P., Sharykin, N.K., Zhouck, I.N.: 1978, Astrophys. and Space Sci. 54, 3 (doi: 10.1007/BF00637902).

Brazhenko, A.I., Melnik, V.N., et al.: 2015, RadioPhys. Radioastron. 20, 10 (in Russian).

Cane, H. V., Erickson, W. C., Prestage, N. P.: 2002, J. Geophys. Res. 107, A101315(doi: 10.1029/2001JA000320).

Gibson, S.E., Kucera, T.A., et al.: 2010, Astrophys. J. 724, 1133(doi: 10.1088/0004-637X/724/2/1133).

Gopalswamy, N.: 2010, in Planetary Radio Emissions VII, H.O. Rucker, W. S. Kurth, P. Louarn, and G. Fischer, Eds. Austrian Academy of Sciences Press, Vienna, pp. 325-342.

Mel'nik, V.N., Konovalenko, A.A., et al.: 2004, Solar Phys. 222, 151(doi: 10.1023/B:SOLA.0000036854.66380.a4).

Melnik, V. N., Rucker, H. O., et al.: 2010, Proceedings of the 7th International Workshop on Planetary, Solar and Heliospheric Radio Emissions (PRE VII), held at Graz, Austria, September 15-17, 2010, pp. 343-350.

Melnik, V.N., Brazhenko, A.I., et al.: 2014, Solar Phys. 289, 263(doi: 10.1007/s11207-013-0328-2).

Stanislavsky, A.A., Konovalenko, A.A., et al.: 2015, Solar Phys. 290, 205(doi: 10.1007/s11207-014-0620-9).

Thejappa, G., MacDowall, R.J.: 2010, Astrophys. J. 720, 1395(doi: 10.1088/0004-637X/720/2/1395).